Intravitreal HDAC Inhibitor Belinostat Effectively Eradicates Vitreous Seeds Without Retinal Toxicity In Vivo in a Rabbit Retinoblastoma Model

Jessica V. Kaczmarek,[1,*] Carley M. Bogan,[1] Janene M. Pierce,[1] Yuankai K. Tao,[2] Sheau-Chiann Chen,[3,4] Qi Liu,[3,4] Xiao Liu,[3,4] Kelli L. Boyd,[4,5,†] M. Wade Calcutt,[6] Thomas M. Bridges,[7] Craig W. Lindsley,[7] Debra L. Friedman,[4,8] Ann Richmond,[4,9–11] and Anthony B. Daniels[1,4,11,12]

[1]Division of Ocular Oncology and Pathology, Department of Ophthalmology and Visual Sciences, Vanderbilt University Medical Center, Nashville, Tennessee, United States
[2]Department of Biomedical Engineering, Vanderbilt University, Nashville, Tennessee, United States
[3]Center for Quantitative Sciences, Vanderbilt University Medical Center, Nashville, Tennessee, United States
[4]Vanderbilt-Ingram Cancer Center, Vanderbilt University Medical Center, Nashville, Tennessee, United States
[5]Department of Pathology, Microbiology and Immunology, Vanderbilt University Medical Center, Nashville, Tennessee, United States
[6]Department of Biochemistry, Vanderbilt University, Nashville, Tennessee, United States
[7]Warren Center for Neuroscience Drug Discovery at Vanderbilt, Department of Pharmacology, Vanderbilt University, Nashville, Tennessee, United States
[8]Department of Pediatrics, Vanderbilt University Medical Center, Nashville, Tennessee, United States
[9]Tennessee Valley Healthcare System, Department of Veterans Affairs, Nashville, Tennessee, United States
[10]Department of Pharmacology, Vanderbilt University, Nashville, Tennessee, United States
[11]Program in Cancer Biology, Vanderbilt University, Nashville, Tennessee, United States
[12]Department of Radiation Oncology, Vanderbilt University Medical Center, Nashville, Tennessee, United States

Correspondence: Anthony B. Daniels, Vanderbilt Eye Institute, Vanderbilt University Medical Center, 2311 Pierce Avenue, Nashville, TN 37232, USA; anthony.b.daniels@vumc.org.

*Current affiliation: Department of Medicine, Baylor College of Medicine, Houston, Texas, United States
†Current affiliation: Gilead Sciences, Inc., Foster City, California, United States

Received: October 1, 2020
Accepted: July 21, 2021
Published: November 10, 2021

Citation: Kaczmarek JV, Bogan CM, Pierce JM, et al. Intravitreal HDAC inhibitor belinostat effectively eradicates vitreous seeds without retinal toxicity in vivo in a rabbit retinoblastoma model. *Invest Ophthalmol Vis Sci.* 2021;62(14):8. https://doi.org/10.1167/iovs.62.14.8

Purpose. Current melphalan-based regimens for intravitreal chemotherapy for retinoblastoma vitreous seeds are effective but toxic to the retina. Thus, alternative agents are needed. Based on the known biology of histone deacetylases (HDACs) in the retinoblastoma pathway, we systematically studied whether the HDAC inhibitor belinostat is a viable, molecularly targeted alternative agent for intravitreal delivery that might provide comparable efficacy, without toxicity.

Methods. In vivo pharmacokinetic experiments in rabbits and in vitro cytotoxicity experiments were performed to determine the 90% inhibitory concentration (IC_{90}). Functional toxicity by electroretinography and structural toxicity by optical coherence tomography (OCT), OCT angiography, and histopathology were evaluated in rabbits following three injections of belinostat 350 µg (2× IC_{90}) or 700 µg (4× IC_{90}), compared with melphalan 12.5 µg (rabbit equivalent of the human dose). The relative efficacy of intravitreal belinostat versus melphalan to treat WERI-Rb1 human cell xenografts in rabbit eyes was directly quantified. RNA sequencing was used to assess belinostat-induced changes in RB cell gene expression.

Results. The maximum nontoxic dose of belinostat was 350 µg, which caused no reductions in electroretinography parameters, retinal microvascular loss on OCT angiography, or retinal degeneration. Melphalan caused severe retinal structural and functional toxicity. Belinostat 350 µg (equivalent to 700 µg in the larger human eye) was equally effective at eradicating vitreous seeds in the rabbit xenograft model compared with melphalan (95.5% reduction for belinostat, $P < 0.001$; 89.4% reduction for melphalan, $P < 0.001$; belinostat vs. melphalan, $P = 0.10$). Even 700 µg belinostat (equivalent to 1400 µg in humans) caused only minimal toxicity. Widespread changes in gene expression resulted.

Conclusions. Molecularly targeted inhibition of HDACs with intravitreal belinostat was equally effective as standard-of-care melphalan but without retinal toxicity. Belinostat may therefore be an attractive agent to pursue clinically for intravitreal treatment of retinoblastoma.

Keywords: retinoblastoma, histone deacetylase inhibitor, HDAC, HDAC inhibitors, belinostat, chemotherapy, intravitreal chemotherapy, animal models, toxicity, efficacy, pharmacokinetics, vitreous seeds, ocular tumors

The introduction of intra-arterial chemotherapy (IAC)[1] and direct intravitreal injections of chemotherapy[2,3] has revolutionized the management of children with advanced intraocular retinoblastoma (RB), as vitreous seeds historically have been the most difficult feature of retinoblastoma to eradicate.[4,5] Previous studies have suggested that intravenous chemotherapy (IVC) salvages only ~30% to 40% of eyes with vitreous seeds,[6–8] and IAC only cures about two-thirds of eyes with vitreous seeds.[9] In contrast, the addition of adjuvant intravitreal injections has been shown to increase efficacy and globe salvage following treatment with either IVC or IAC.[9–13]

Currently, the backbone of current standard-of-care chemotherapeutic regimens used for both IAC and intravitreal chemotherapy is melphalan. However, there is extensive evidence in both animals[14–16] and patients[16–19] that melphalan is highly toxic to the retina. Thus, although effective, intravitreal melphalan regimens cause damage to retinal function and affect residual vision, which can cause significant morbidity in a disease that often presents bilaterally.

Alternative agents to melphalan have been explored for both the intra-arterial and intravitreal routes. However, these alternative drugs used intravitreally have generally either repurposed already-used intravenous agents (e.g., carboplatin, etoposide)[20,21] or simply repurposed already-used intra-arterial agents (e.g., topotecan).[22–24] These have generally first been tried clinically, without first being tested in preclinical studies to demonstrate efficacy or lack of toxicity or to inform dosing decisions.

Our recently described retinoblastoma tumor model[25] and toxicity assessment platform[14] allow both the efficacy and toxicity of novel compounds to be studied, thus aiding in preclinical assessment of novel intravitreal (and intra-arterial) chemotherapeutic agents. Various histone deacetylases (HDACs) are known to complex with the retinoblastoma protein (pRB)[26,27] or other similar retinoblastoma family pocket proteins[28,29] and to have an effect on pRB pathway-regulated genes.[29–31] However, it is unclear whether this approach would be effective in tumor cells in which RB protein function is already abrogated. Given that RB loss is a hallmark of many different solid tumors,[32] this has implications for other cancer types, as well. We therefore explored the utility of HDAC inhibition as an alternative strategy to eradicate retinoblastoma vitreous seeds using our RB xenograft model[25] to assess efficacy in vivo, and we assessed the ocular toxicity of this agent in vivo using the toxicity assessment platform that we have developed.[14] We demonstrate that the pan-HDAC inhibitor belinostat is equally effective to standard-of-care melphalan, but it does not cause the retinal functional loss seen with melphalan, thus suggesting that it may be an attractive alternative agent.

Methods

Statement of Research Ethics

All animal experiments were performed under the auspices of the Vanderbilt Institutional Animal Care and Use Committee (approved protocol ID #M1800146) and adhered to the ARVO Statement for the Use of Animals in Ophthalmic and Vision Research.

Belinostat Intravitreal Pharmacokinetics

New Zealand White rabbits (2.8–3.0 kg) were used for all studies. One microgram belinostat (Acrotech Biopharma, East Windsor Township, NJ, USA) in 50 µL saline was injected 2 to 3 mm posterior to the limbus into the vitreous cavity ($n = 4$ rabbits). Serial vitreous taps were then performed through a 20-gauge valved vitrectomy cannula that had been inserted 2 to 3 mm behind the limbus on the other side of the eye. Samples were obtained at 15 minutes, 30 minutes, 1 hour, 2 hours, 4 hours, and 6 hours after injection. Preplacement of a valved cannula maintained the stability of the eye and prevented efflux of vitreous contents during manipulations. Vitreous samples were immediately placed on dry ice and then stored at –80°C.

Similar to previous studies,[25,33] vitreous samples were thawed and spiked with an internal carbamazepine standard, diluted with blank plasma, and deproteinized with acetonitrile. Calibration samples were prepared in parallel by spiking blank plasma with internal standard and known concentrations of belinostat. Samples were analyzed on a Thermo TSQ Quantum Ultra mass spectrometer (Thermo Fisher Scientific, Waltham, MA, USA) interfaced to a Waters ACQUITY UPLC system (Waters, Milford, MA, USA).

Belinostat concentrations were averaged across rabbits at each time point, and the resulting mean time–concentration data from each matrix were analyzed via non-compartmental analysis (Phoenix WinNonlin 6.4; Certara, Princeton, NJ, USA) to determine pharmacokinetic parameters, including half-life.

In Vitro Determination of Dosing

Human WERI-Rb1 retinoblastoma cells were grown in RPMI with 10% fetal bovine serum under normal growth conditions, as reported previously.[24,33] Five thousand cells were plated in 96-well plates and exposed to belinostat at various concentrations for 4 hours (equivalent to 5 half-lives as determined through the above-described pharmacokinetic experiments). The belinostat-containing media were then removed and replaced with fresh media. After 7 days, live cells were counted using the CellTiter-Blue assay (Promega, Madison, WI, USA). Survival curves were graphed with Prism (GraphPad, San Diego, CA, USA), and the 50% inhibitory concentration (IC_{50}) and 90% inhibitory concentration (IC_{90}) were calculated. We then back-calculated, using the pharmacokinetic parameters determined above, the dose of belinostat that would have had to have been initially injected into the eye to obtain a concentration above the theoretical IC_{90} concentration in the vitreous on the opposite side of the eye for a duration of 5 half-lives.[33]

Assessment of Ocular Toxicity and Determination of Maximum Tolerable Dose of Intravitreal Belinostat In Vivo in Rabbits

Intravitreal injections of belinostat were given into non–tumor-bearing rabbit eyes weekly for 3 weeks. We used various doses of belinostat to determine the maximum tolerable dose, including the injection dose that would achieve 2× IC_{90} (350 µg) or 4× IC_{90} (700 µg; see Results section for calculation of IC_{90}). Additional cohorts of rabbits received equivalent volumes of saline injections as a control, or received melphalan 12.5 µg as a comparator of the toxicity associated with current standard-of-care treatment. Because the rabbit vitreous volume is half the size of a human child's vitreous volume, experiments with intravitreal injections in rabbits generally have used a dose equal

Investigative Ophthalmology & Visual Science

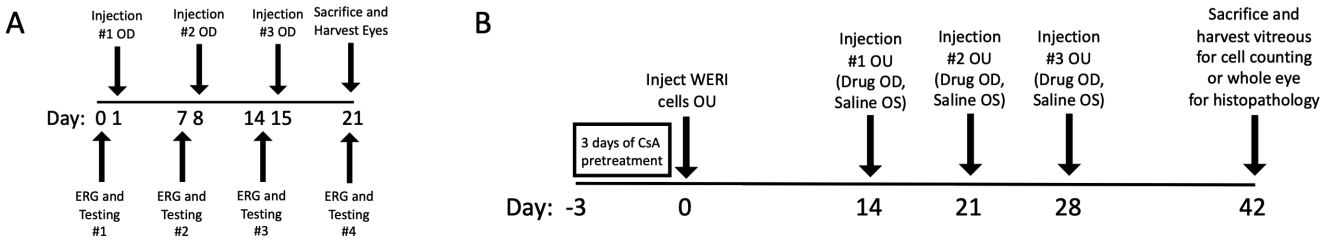

Figure 1. Experimental design of toxicity and efficacy experiments in the rabbit model. (**A**) Toxicity experiments. Drug (belinostat, melphalan, or saline, depending on the cohort) was injected into the right eye of New Zealand White rabbits once per week for 3 consecutive weeks. One day prior to each injection, functional and structural testing was obtained (see Methods section). One week following the final (third) injection, testing was again performed, and then the rabbits were euthanized and globes harvested for histopathologic evaluation. (**B**) Efficacy experiments. Following 3 days of cyclosporine (CsA) immunosuppression (which also continued throughout the course of the experiment), WERI-Rb1 cells were injected into the vitreous of both eyes of New Zealand White rabbits. After 2 weeks of growth, once-per-week injections of drug (belinostat 350 µg or melphalan 12.5 µg) were given into the right eye (OD) and saline into the left eye (OS). Imaging was obtained and rabbits were sacrificed 2 weeks after completing the three (weekly) injections.

to half that used in patients,[24,33–35] and we have maintained that accepted conversion factor in these experiments. In our study, 12.5 µg represents the rabbit vitreous volume-adjustment of the clinical dose in humans (25 µg). Thus, there were four total cohorts: belinostat 350 µg (2× IC_{90}), belinostat 700 µg (4× IC_{90}), melphalan 12.5 µg, and saline. Each cohort consisted of 7–11 rabbits. For each rabbit, only one eye was treated and evaluated in the toxicity assessment experiments.

Figure 1A shows a diagrammatic representation of the experimental design. Testing was obtained at baseline and prior to each week's injection and then 1 week after the final (third) injection (immediately prior to sacrificing the rabbit and harvesting the eye). Retinal structure and function were assessed with our previously described toxicity assessment platform.[14,33] Briefly, testing consisted of electroretinography (ERG), clinical ophthalmic examination, fundus photography, optical coherence tomography (OCT), and OCT angiography (OCTA). OCT and OCTA were performed using a custom-built, 780-nm spectral-domain engine and ophthalmic scanner.[14,36] Intravitreal injections were performed weekly and always within 1 day following testing. In addition, after rabbits were sacrificed, the eyes were harvested and fixed in Davidson's solution (as described above), and histologic sections were evaluated by an experienced veterinary pathologist (KLB).

For ERG testing, following pupillary dilation, rabbits were dark adapted for at least 1 hour, and then anesthesia was induced with ketaset and xylazine. The ground and reference stainless steel subdermal needle electrodes (OcuScience, Henderson, NV, USA) were inserted subcutaneously on the top of the head and at the base of the ear, respectively. The corneal Gold Mylar Film electrode (OcuScience) was then centered on the cornea after placing a small drop of Goniovisc (OcuScience) on the concave side of the contact lens. ERG was performed using the Handheld Multi-species Electroretinography (HMsERG) Model 2000 (OcuScience) under a Faraday cage, according to the modified International Standard for Clinical Electrophysiology of Vision protocol for rabbits.[37] Specific testing conditions were as follows: scotopic 100-mcd.s/m^2 flash intensity, scotopic 3000-mcd.s/m^2 flash intensity, scotopic 10,000-mcd.s/m^2 flash intensity, 10 minutes of light adaptation followed by photopic 3000-mcd.s/m^2 flash intensity (with background of 30,000 mcd/m^2), and 30-Hz flicker with 3000-mcd.s/m^2 flash intensity.

For assessment of retinal function by ERG, toxicity was defined for each rabbit for each test and each parameter (e.g., rabbit 1, scotopic 100 A-wave amplitude; rabbit 2, photopic 3000 B-wave implicit time). Toxicity was defined prospectively as described previously.[14,24,33,35] Briefly, toxicity was deemed significant for a given dose in a rabbit group if there was a 25% reduction in average ERG amplitude or a 25% prolongation of average implicit time for a given parameter when comparing the post-treatment values with the pre-treatment values, and the difference was statistically significant. For assessment of toxicity in individual rabbits, toxicity was defined as a 25% reduction in ERG amplitude or a 25% prolongation of implicit time for a given parameter when comparing the post-treatment values with the pre-treatment values for that rabbit.

Assessment of Efficacy of Intravitreal Belinostat for Vitreous Seeds In Vivo in Rabbits

A representation of the experimental design is shown in Figure 1B. Retinoblastoma vitreous seeds were generated by injection of 1,000,000 WERI-Rb1 cells in 100 µL saline into the vitreous of both eyes of cyclosporine-immunosuppressed rabbits, as we have described previously.[25,33] After 2 weeks of vitreous seed growth, rabbits were treated with three injections, one injection per week, of 350 µg/100 µL belinostat (right eye) and 100 µL saline (left eye). The 350-µg injection was selected because it represented the maximum tolerable dose as determined from the toxicity experiments (see above and also Results section). In order to compare the efficacy of intravitreal belinostat against standard-of-care melphalan, an additional cohort of rabbits was treated with 12.5 µg/100 µL melphalan (right eye) and 100 µL saline (left eye). As explained above, 12.5 µg represents the rabbit vitreous volume-adjusted equivalent of the clinically used dose in humans (25 µg).

Two weeks after the third and final intravitreal injection, the rabbits were sacrificed and the eyes harvested. The vitreous of each eye was then harvested in toto and dissolved, and live cells were counted by direct microscopic counting using trypan blue. In four additional rabbits per cohort, the entire eye was harvested and submitted for histopathology, either 2 weeks after the first injection (n = 2 rabbits per cohort) or 2 weeks after the third injection (n = 2 rabbits per cohort).

Investigative Ophthalmology & Visual Science

Statistical Analyses of Rabbit Efficacy Data and ERG Data

For the efficacy experiments, the paired *t*-test was used to evaluate the mean difference in cell numbers on a square root scale between the correlated samples (left saline-treated eyes and right drug-treated eyes). The data were transformed to better meet normality assumptions. To compare the efficacy of belinostat to melphalan, the relative reduction of cell counts was analyzed to determine differences between the two independent groups using the Welch two-sample *t*-test. To evaluate the toxicity at different dosages, a linear mixed-effects model was fitted with the repeated measurement (pre- or post-treatment) for each ERG parameter and each test.[33] Using model-based (least-square) means, the average change from pre- versus post-treatment and the difference in change among the different treatment groups (difference of differences) were estimated and compared with the Wald test. The definition of toxicity for a treatment was defined as above. Bonferroni adjusted *P* values were reported to account for multiple comparisons among groups. All tests were two sided, with adjusted *P* values < 0.05 considered statistically significant. The analyses were performed using R 3.6.3 (R Foundation for Statistical Computing, Vienna, Austria), including the packages "nlme" and "emmeans."

Real-Time Glo Annexin V Apoptosis and Necrosis Assay

It has been suggested that HDACs mediate cell death in cancer cells via both apoptotic and non-apoptotic mechanisms.[38,39] To assess the relative amount of apoptosis as a proportion of total cell death following belinostat treatment, we performed the dual luminescence-fluorescence Real-time Glo Annexin V Apoptosis and Necrosis Assay (JA1011; Promega), according to the manufacturer's protocol. Briefly, 10,000 WERI-Rb1 cells were plated in each well of a 96-well plate and grown for 3 days. After 3 days, 16-µM (2× IC_{90}) belinostat (Selleck Chemical, Houston, TX, USA) was added to wells designated as treated, and detection reagents were added to all wells of the plate, including wells containing only cells and wells containing only media. Plates were read every 2 hours for a total of 72 hours with a SpectraMax iD3 Multi-Mode Microplate Reader (Molecular Devices, San Jose, CA, USA).

RNA Sequencing

WERI-Rb1 cells were grown in flasks for 3 days, and 16-µM (two times the calculated IC_{90}) belinostat (Selleck Chemical) was added to each flask after the 3 days. Three million cells were collected at each time point, spun down, and resuspended in 300 µL RNAProtect solution (QIAGEN, Hilden, Germany), and kept at –20°C until RNA isolation. Cells were removed from the RNAProtect solution by centrifugation at 10,000 rpm and processed using the QIAGEN RNeasy Mini Kit following the manufacturer's protocol. DNAse treatment was performed, and the RNA was eluted in 30 µL water. RNA sequencing (RNA-seq) libraries were prepared using 200 ng of total RNA and the NEBNext Ultra II Directional RNA Library Prep With Sample Purification Beads from Illumina (E7765; New England BioLabs, Ipswich, MA, USA) per the manufacturer's instructions. This kit employs strand-specific/directional methods for sequencing RNA to provide information on the DNA strand from which the RNA strand was transcribed. The libraries were sequenced using the NovaSeq 6000 with 150-bp paired-end reads targeting 50 million reads per sample. RTA 2.4.11 (Illumina, San Diego, CA, USA) was used for base calling and analysis used MultiQC v1.7. Adapters were trimmed by Cutadapt (https://github.com/marcelm/cutadapt). After trimming, RNAseq reads were mapped to the human reference genome GRCh38 using STAR and quantified by FeatureCounts. DESeq2 was used to detect differential expression between treated and untreated samples. Genes with a fold change of >2 and a false discovery rate < 0.05 were considered to be significantly differentially expressed. Functional enrichment analysis was performed against gene ontology and the KEGG database using WebGestalt and gene set enrichment analysis (GSEA).

Results

Belinostat Pharmacokinetics and In Vitro Determination of Expected Effective In Vivo Dose

After an injection of 1 µg belinostat, the peak concentration at the opposite side of the eye was achieved at 30 minutes post-injection (Fig. 2A). The vitreous half-life of belinostat was 0.8 hours. The average C_{max} at the opposite side of the eye was 0.457 µg/mL at 30 minutes. Compared with the theoretical C_{max} of 0.71 µg/mL (calculated as 1 µg/1.4 mL), which would be achieved with instantaneous diffusion of 1 µg of belinostat into a theoretical average rabbit vitreous volume of 1.4 mL, this actual C_{max} at the opposite side of the eye achieved 30 minutes after injection was therefore ~64% of the expected C_{max}. This represents the minimum amount of peak drug concentration available to treat retinoblastoma vitreous seeds located at the farthest point in the eye relative to the injection site. This is presumably due to rapid efflux of the drug during this time period of distribution of belinostat across the vitreous. This is plausible, as the peak was achieved at 30 minutes (approximately 63% of one 0.8-hours half-life). Mathematically, one would expect 65% of the drug to remain after 0.63 half-lives, which is exceptionally close to the 64% that was actually measured empirically.

Given that retinoblastoma vitreous seeds would be expected to experience exposure to a drug for only a limited period of time, which is dictated by pharmacokinetics and drug half-life in the vitreous, we next determined the in vitro IC_{90} of belinostat based on this empiric exposure time. The half-life of belinostat in the rabbit eye was calculated at 0.8 hours. Thus, we determined the minimum amount of WERI-Rb1 human retinoblastoma cells that would be expected to be killed following 5 half-lives of exposure (~4 hours). The fraction of WERI-Rb1 cells still alive 7 days after this brief exposure was determined for different drug concentrations. The IC_{90} of WERI-Rb1 cells following a brief 4-hour exposure to belinostat was calculated at 8 µM belinostat (Fig. 2B). We then back-calculated that this minimum IC_{90} concentration would be achieved for a full 5 half-lives at the opposite side of the rabbit eye following intravitreal injection of ~175 µg belinostat.

Retinal Functional Toxicity of Various Doses of Intravitreal Belinostat Compared With Melphalan in Rabbits

The toxicity associated with various concentrations of belinostat was evaluated to determine the maximum tolerable

Investigative Ophthalmology & Visual Science

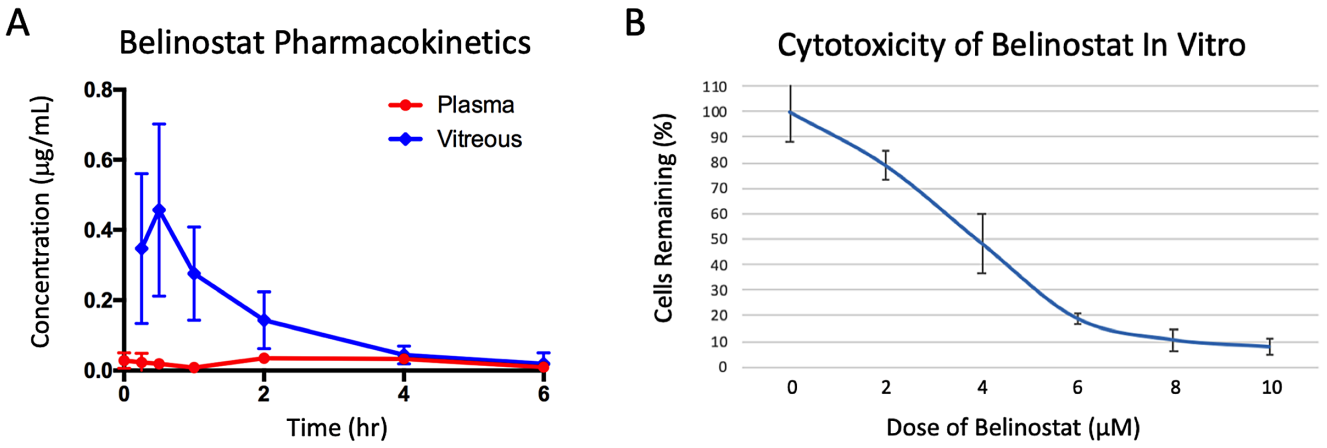

Figure 2. Pharmacokinetics of intravitreal belinostat in vivo in the rabbit eye and dose-dependent survival curves of retinoblastoma cells to transient exposure to belinostat in vitro. (**A**) Pharmacokinetic curve in the rabbit vitreous following intravitreal injection of 1 µg of belinostat. Sampling was performed through a valved vitrectomy cannula inserted on the contralateral side of the eye relative to the injection site, and all sampling was performed on the far side of the vitreous relative to the injection site. The use of a valved vitrectomy cannula helped to maintain eye stability and prevent leakage throughout the course of the experiment. (**B**) CellTiter-Blue survival curve in vitro of human WERI-Rb1 cells exposed to various doses of belinostat for 4 hours (equal to 5 vitreous half-lives). Surviving cells were measured at the 7-day time point. The IC_{90} can be found to correspond to 8 µM belinostat for this length of exposure.

dose. Doses studied included 2× IC_{90} (350 µg, equivalent to 700 µg in the larger human vitreous) and 4× IC_{90} (700 µg, equivalent to 1400 µg in humans). These belinostat doses were compared with a clinically used, effective dose of melphalan (12.5 µg in the rabbit, equivalent to 25 µg in humans), as well as to saline as a control for the repeated injection procedures. The primary quantitative outcome was ERG measurements over the course of treatment (see Methods section).

Although the saline control groups experienced no worsening of ERG parameters, three weekly injections of melphalan caused significant worsening of almost all ERG parameters, with reductions in ERG amplitudes between 48% and 84%. These reductions were highly statistically significant (Fig. 3). When individual rabbits were examined, rather than just the averages across the melphalan cohort, we found that every melphalan-treated rabbit experienced worsening of ERG parameters, affecting a median of nine (interquartile range, 8–10) out of a total of 18 different measured parameters. Similar results were found when considering implicit time prolongation. Representative ERG tracings are available in the Supplementary Material.

In contrast, rabbits treated with belinostat 350 µg (twice the dose calculated to achieve the IC_{90} on the opposite side of the rabbit vitreous for 5 half-lives) did not experience any statistically or clinically meaningful worsening of ERG parameters (Fig. 3). Even at 4× IC_{90} (700 µg, equivalent to 1400 µg in patients), only a few parameters showed signs of much milder retinal functional loss (Fig. 3). Because 350 µg (2× IC_{90}) did not cause any retinal functional toxicity, this was determined to be the maximum tolerable dose and was used in subsequent efficacy experiments.

Comparison of Retinal Structural Changes Between Belinostat-Treated and Melphalan-Treated Eyes

Eyes treated with three weekly injections of belinostat showed no retinal damage and were histologically indistinguishable from saline-treated control eyes or untreated eyes (Fig. 4). This was true even for those eyes treated with twice the clinically effective dose (700 µg, equivalent to 1400 µg in patients). In contrast, retinas from eyes treated with the clinically effective dose of melphalan (12.5 µg, equivalent to 25 µg in patients) all demonstrated severe atrophy (Fig. 4).

OCT showed retinal thinning similar to what was ultimately seen on histopathology, with normal-appearing retinal layers and thickness in belinostat-treated eyes and severe thinning and loss of normal layers in melphalan-treated eyes. OCTA showed severe vascular pruning in melphalan-treated eyes but not in contralateral untreated eyes or saline-treated controls (Fig. 5). In contrast, almost all belinostat-treated eyes, in both the 350-µg cohort and the 700-µg cohort, showed normal and full retinal microvasculature. The exception was a single belinostat-treated eye in which there was some vascular pruning noted only in the vessels on the side nearest the injection site. With melphalan, a similar, but much more profound, dose-related toxicity gradient has also been seen, both in rabbits and human patients.[35]

Lens Findings in Belinostat-Treated Eyes

All eyes treated with belinostat developed a translucent, mid-peripherally located "plaque"-like area on the posterior lens capsule on the side near the injection site (Fig. 6). This was seen in all belinostat-treated eyes, but in none of the saline-treated or melphalan-treated eyes, and so does not represent iatrogenic needle trauma to the lens. Careful histopathologic investigation of the entire posterior capsule in these eyes failed to demonstrate any microscopically or histologically observable pathology.

Relative Efficacy of Intravitreal Belinostat and Melphalan to Treat Retinoblastoma Vitreous Seeds In Vivo in Rabbits

Rabbits harboring WERI-Rb1–derived vitreous seeds in both eyes were treated with either belinostat or melphalan in

Investigative Ophthalmology & Visual Science

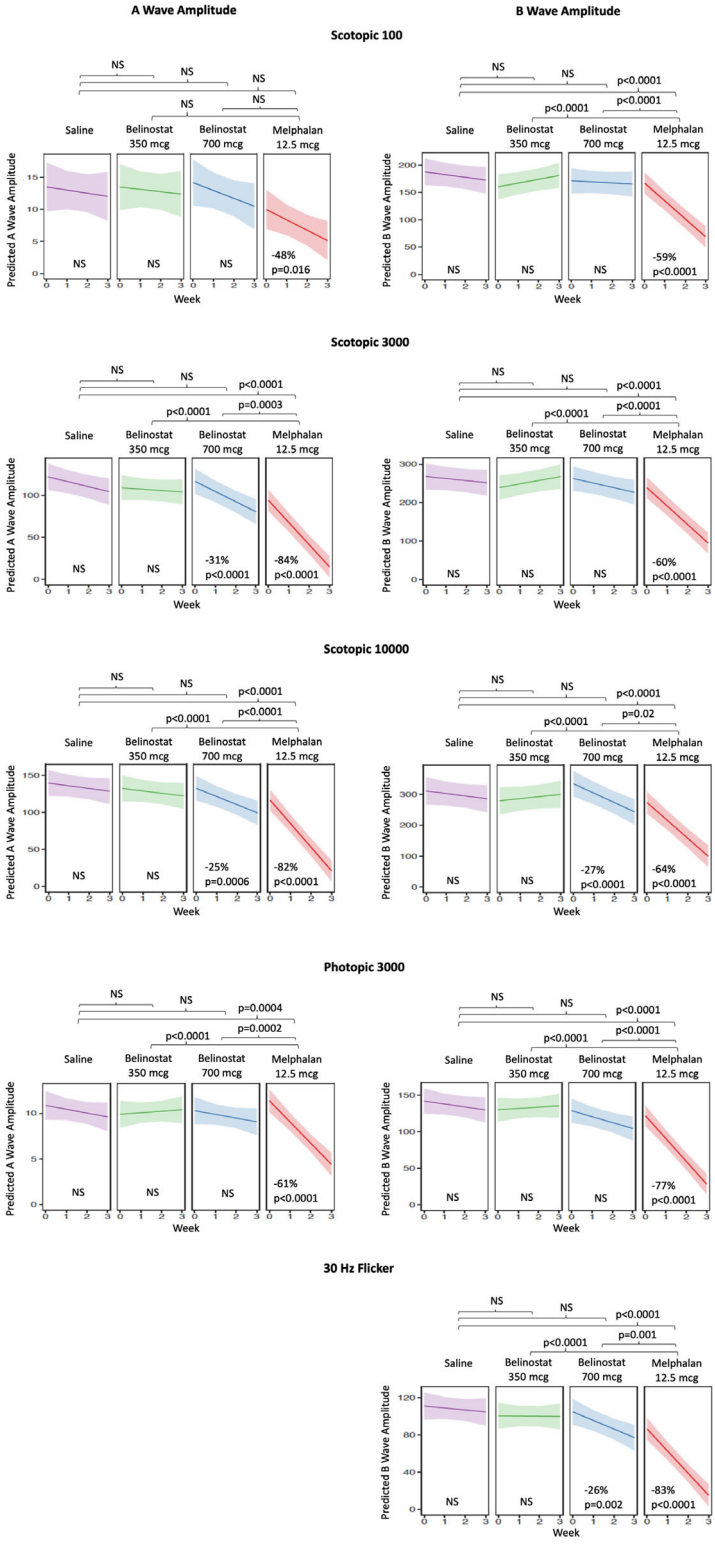

Figure 3. Functional retinal toxicity of various doses of intravitreal belinostat versus melphalan. Electroretinography was performed weekly, 1 day prior to each of the three planned injections, as well as 1 week after the final injection (immediately prior to sacrificing the rabbit). Retinal responses to scotopic 100-mcd.s/m^2 flashes, scotopic 3000-mcd.s/m^2 flashes, scotopic 10,000-mcd.s/m^2 flashes, photopic 3000-mcd.s/m^2 flashes, and 30-Hz flicker flashes were recorded. A-wave and B-wave amplitudes and A-wave and B-wave implicit times were recorded (except for with the 30-Hz flicker, where there is only a B wave). *Shaded areas* on the graphs represent 95% confidence intervals. No toxicity (see Methods section for toxicity criteria) was observed for any parameter in the saline-treated control eyes or in the cohort treated with 350 µg of belinostat. However, significant toxicity was seen for every parameter in the cohort of rabbits treated with 12.5 µg of melphalan. With 700 µg belinostat (equal to twice the clinically effective dose), a few parameters showed mild toxicity. Graphs of amplitudes are shown, but similar results were seen for implicit times, as well. For those particular tests where significant toxicity was seen, percent change and *P* values for estimates of trend are shown along with the particular graph. *P* values of the differences among groups are shown at the top of each graph. NS, not significant.

Investigative Ophthalmology & Visual Science

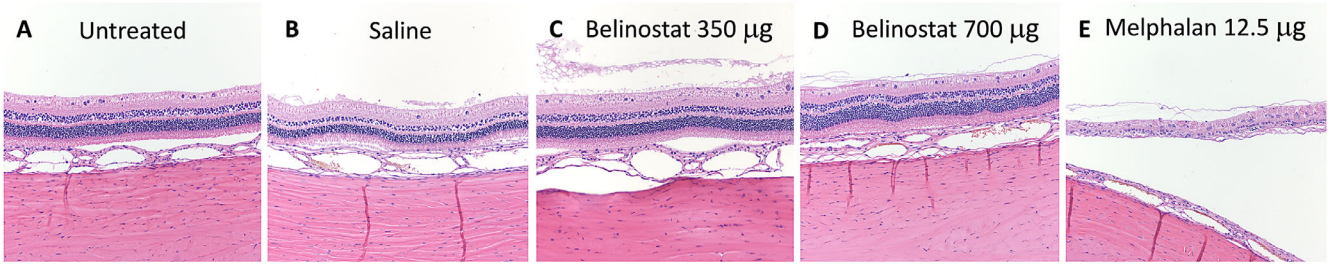

Figure 4. Absence of structural retinal toxicity in belinostat-treated eyes compared with melphalan. Histopathology demonstrated normal retinal architecture in untreated eyes (**A**) and in the saline-treated eyes (**B**). Eyes treated with intravitreal injections of 350 µg belinostat (**C**) or 700 µg belinostat (**D**) were both histologically indistinguishable from saline-treated (or untreated) eyes. (**E**) In contrast, eyes treated with 12.5 µg melphalan showed significant retinal atrophy on histopathology.

the right eye and saline in the left eye. Following three weekly injections of 350 µg belinostat (equivalent to 700 µg in humans), 95.5% of cells were killed, compared with the contralateral eye treated with intravitreal saline injections ($P < 0.001$) (Fig. 7). Following three weekly injections of melphalan at a dose known to be clinically effective (12.5 µg, equivalent to 25 µg in humans), 89.4% of cells were killed, compared with the contralateral eye treated with intravitreal saline injections ($P < 0.001$). Therefore, belinostat was just as effective as melphalan, with no statistically significant difference between the 95.5% of cells killed by belinostat and the 89.4% of cells killed by melphalan ($P = 0.10$) (Fig. 7).

For additional rabbits ($n = 4$ rabbits per treatment cohort) treated as above with belinostat, melphalan, or saline, the entire eyes were harvested and submitted for histopathology. These demonstrated comparably few residual cells in both the belinostat-treated eyes and the melphalan-treated eyes, 2 weeks after three injections (Figs. 7E–7G). TUNEL staining was performed, and this confirmed that the few remaining cells in the belinostat-treated eyes were in the process of dying, with no viable cells remaining (Fig. 7H). This suggests that the ~5% of "live" cells counted in the tumor quantitation assay following three injections of belinostat were likely similarly not viable.

Mechanisms of Cell Death and Specific Genes Regulated by Belinostat

To study the specific sets of genes regulated by belinostat treatment, we performed a time-course experiment using RNA-seq of belinostat-treated cells in vitro. Gene expression data demonstrated that pan-HDAC inhibition with belinostat lead to changes in gene expression of a large number of genes, which increased over time from 1412 differentially expressed genes at 2 hours post-treatment (970 upregulated, 442 downregulated) to 7345 differentially expressed genes (4092 upregulated, 3253 downregulated) by 24 hours after treatment. These changes were highly statistically significant, as seen in the volcano plots (Fig. 8).

GSEA demonstrated that the genes that were regulated by belinostat were highly consistent with previous reported gene sets regulated by other pan-HDAC inhibitors in other types of cancer cells.[40–42] Gene ontology studies examining molecular function of the sets of genes differentially expressed following belinostat treatment demonstrated that at early time points (2 and 4 hours), the most commonly regulated genes were those that functioned in transcription itself and in regulation and specificity of gene expression, such as transcriptional activators and repressors and sequence-specific DNA binding. At later time points (6 and 8 hours), the most commonly regulated genes were those that functioned in cell membrane channels and transport and cellular homeostasis. Real-time dual apoptosis/necrosis experiments demonstrated that apoptosis accounts for only part of the total cell death (necrosis) that is ultimately caused by belinostat treatment.

Discussion

Using a series of in vivo pharmacokinetic, efficacy, and toxicity experiments, we demonstrated that intravitreal injection of the pan-HDAC inhibitor belinostat is equally effective at eradicating human retinoblastoma vitreous seed xenografts in vivo as compared with current standard-of-care melphalan, but belinostat does not cause the same retinal toxicity seen with melphalan. We likewise demonstrated that 350 µg belinostat (equivalent to 700 µg in the human eye) appears to be the ideal starting dose to use for intravitreal injection.

Because HDAC inhibitors have never previously been used in clinical practice for the treatment of RB patients, nor have they previously been used by intravitreal injection for any indication in clinical practice, we initially had to determine the intravitreal IC_{90} of belinostat for retinoblastoma cells through a series of in vivo pharmacokinetic and in vitro cytotoxicity experiments. First, the vitreous in rabbits (and in young children) is quite solid, and so we posited that there was a not-insignificant transit time for the drug to cross the vitreous and that during that time of transit some of the drug would be effluxed. Thus, there would be less drug available to treat vitreous seeds located on the far side of the vitreous cavity. We therefore injected into one side of the vitreous, and we measured drug concentration from the other side over time. As expected, there was a reduction in drug concentration on the far side of the eye, with only 64% of the theoretical maximum reaching the other side, and this diffusion across the vitreous took approximately 30 minutes on average to achieve. Second, our previous work with other drugs had demonstrated that intravitreal and intra-arterial injections of various other drugs leads to high but transient vitreous concentrations, with relatively rapid efflux.[24,25] Thus, following intravitreal injection, the vitreous seeds would only be exposed to the initial high concentration very briefly. We therefore determined the vitreous half-life to ensure that the dose calculated for the initial injection would allow a concentration (on the opposite side of the vitreous) above the IC_{90} for a length of time equivalent to at

Investigative Ophthalmology & Visual Science

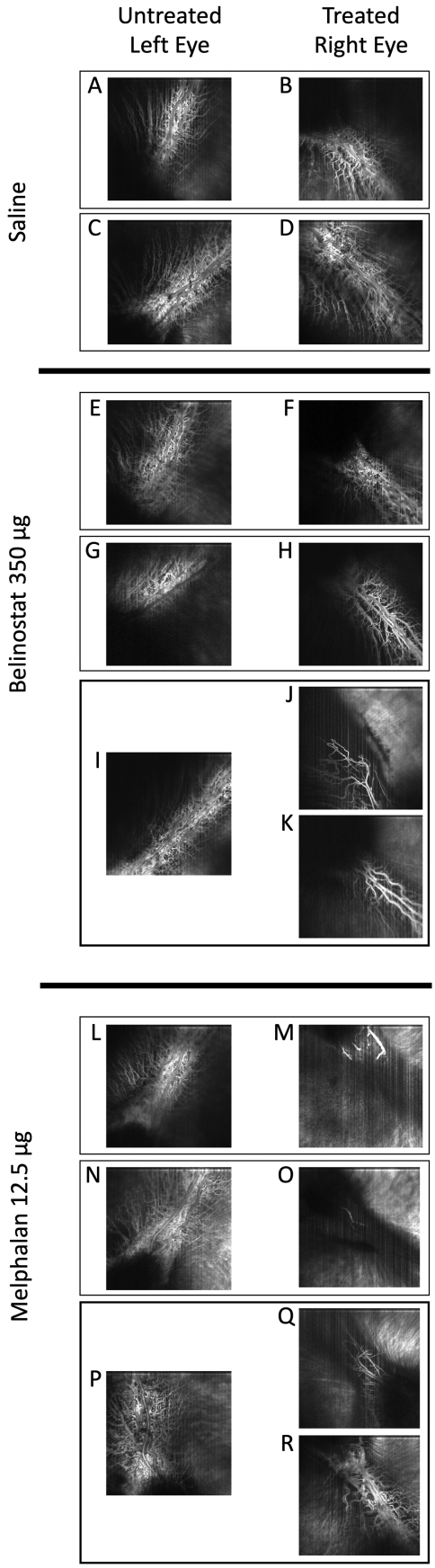

Figure 5. Comparison of retinal microvascular toxicity of various intravitreal agents. OCT and OCTA were performed over the course of treatment with three weekly injections of saline, belinostat, or melphalan. Shown are OCTA images of the treated right eyes and the untreated left control eyes immediately prior to sacrifice 1 week following the third and final injection. (**A–D**) Saline-treated cohort. No retinal microvascular loss was seen in saline-treated right eyes (**B**, **D**), compared with untreated left eyes (**A**, **C**). (**E–K**) Belinostat-treated cohort. No retinal microvascular loss was seen in almost all belinostat-treated right eyes (**F**, **H**), which appeared similar to their contralateral untreated left eyes (**E**, **G**, **I**). In a single eye, some microvascular pruning was noted near the injection site (**J**), where the drug dose would have been greatest before diffusing across the vitreous. The central retina and the retina on the opposite side of the eye were normal (**K**). (**L–R**) Melphalan-treated cohort. Severe loss of microvasculature was seen in all melphalan-treated right eyes (**M**, **O**) compared with the contralateral untreated left eyes (**L**, **N**, **P**). In a single eye, the microvascular loss was noted to be worse on the side of the injection, with some relative sparing of the vessels on the side of the retina farthest from the injection site, where the dose was lower (**Q**, **R**). This is similar to what has been described clinically with melphalan, where there is a gradient effect and greatest toxicity nearest the injection site.

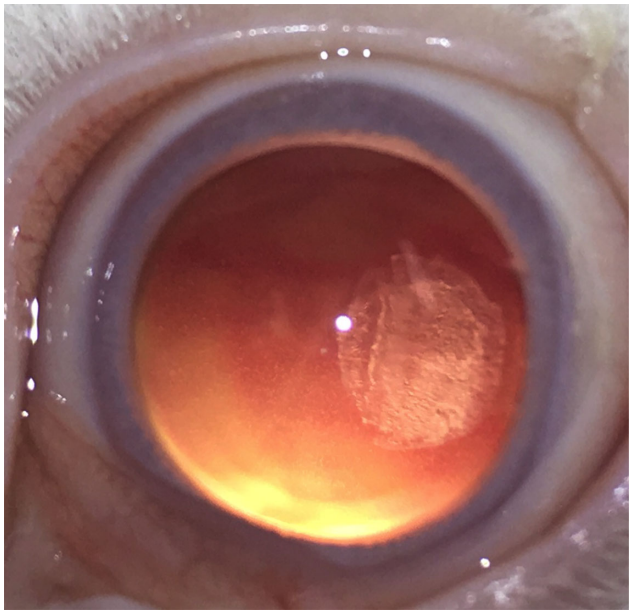

Figure 6. Posterior lens capsule finding in eyes treated with intravitreal belinostat. Eyes treated with a series of three intravitreal belinostat injections (350 µg and 700 µg) developed a translucent plaque-like area in the mid-periphery of the posterior lens capsule on the side nearest the injection site. This was thought to be due to a transiently high local concentration of drug in the adjacent vitreous at the time of injection and is attributed to the relatively large size of the lens relative to the vitreous cavity in rabbits, necessitating injecting very close to the posterior lens capsule. Postmortem pathologic evaluation showed no histopathologic abnormalities of the lens or lens capsule in any of the treated eyes, despite the clinically visible area seen here. This was seen in all belinostat-treated eyes and none of the saline or melphalan-treated eyes, eliminating the possibility that this was due to iatrogenic lens trauma from the needle itself.

Investigative Ophthalmology & Visual Science

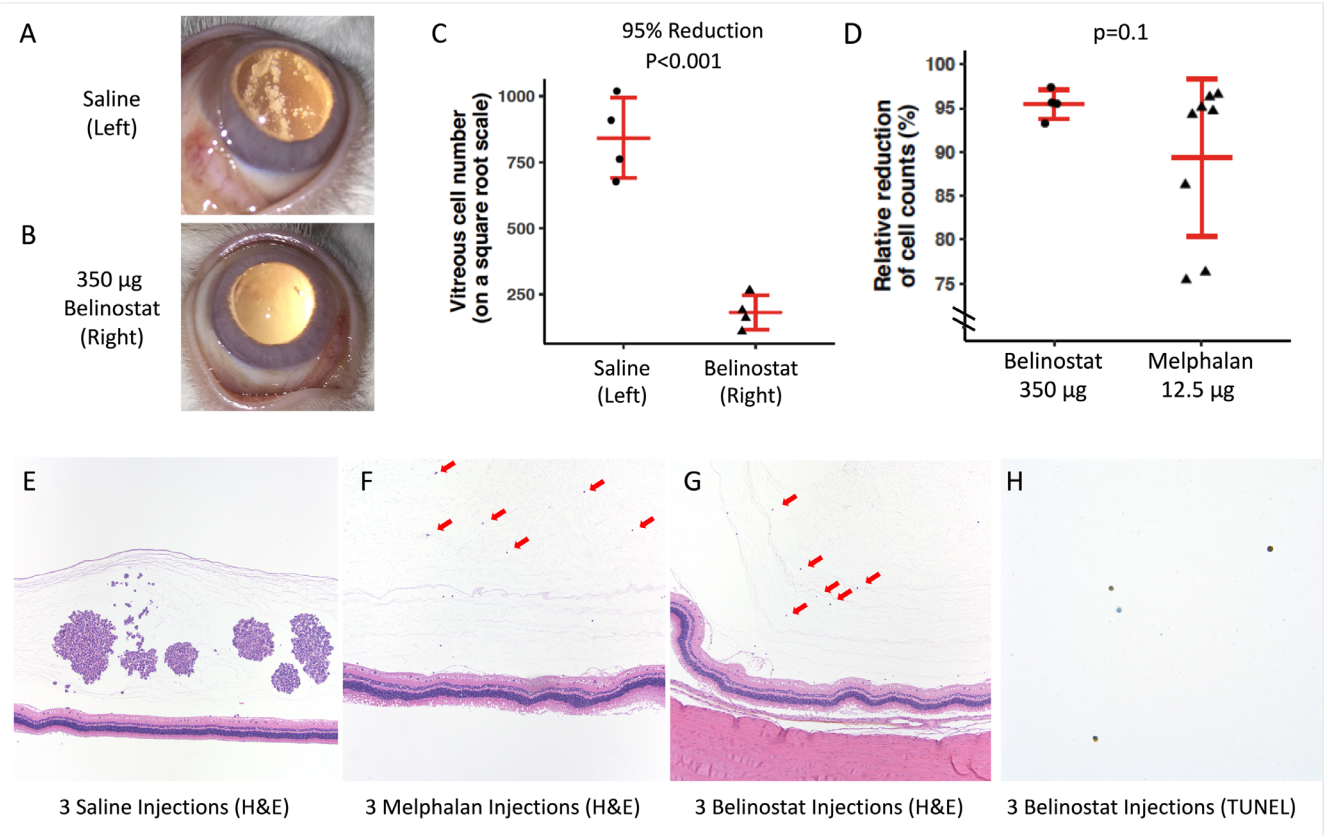

Figure 7. The efficacy of intravitreal belinostat against retinoblastoma vitreous seeds in a rabbit xenograft model. One million WERI-Rb1 human retinoblastoma cells were injected into the vitreous of both eyes of cyclosporine-immunosuppressed rabbits. Following 2 weeks of growth, the eyes were given three weekly injections of intravitreal drug (right eye) or intravitreal saline (left eye). (**A**, **B**) Residual vitreous seeds 2 weeks following the final (third) injection, showing significant large seeds in a representative left (saline-treated) eye (**A**) and complete clinical resolution of the vitreous seeds in a representative belinostat-treated right eye (**B**). (**C**) Quantification of residual live vitreous seeds 2 weeks after the third injection of belinostat (right eyes) or saline (left eyes), showing massive reduction in live tumor cells with belinostat 350 µg. Note that the scale is a square-root scale and is not linear. (**D**) Comparison of relative reduction with belinostat versus melphalan (compared with their respective saline-treated contralateral eyes), demonstrating no statistically significant difference between the two treatments. Note that the *y*-axis extends from 75% to 100%, and the top of the *y*-axis represents the greatest *reduction*. (**E**) Live vitreous seeds in a control eye treated with three injections of saline (hematoxylin and eosin stain, 10× magnification). (**F**) Hematoxylin and eosin stain of an eye treated with three injections of 12.5 µg melphalan, with very few residual cells remaining (arrows, 10× magnification). (**G**) Hematoxylin and eosin stain of an eye treated with three injections of 350 µg belinostat, demonstrating very few residual cells remaining (*arrows*), similar to melphalan (10× magnification). (**H**) TUNEL stain of the same belinostat-treated eye as in **G**, demonstrating that the few residual cells are all undergoing apoptosis, with no viable cells remaining (40× magnification).

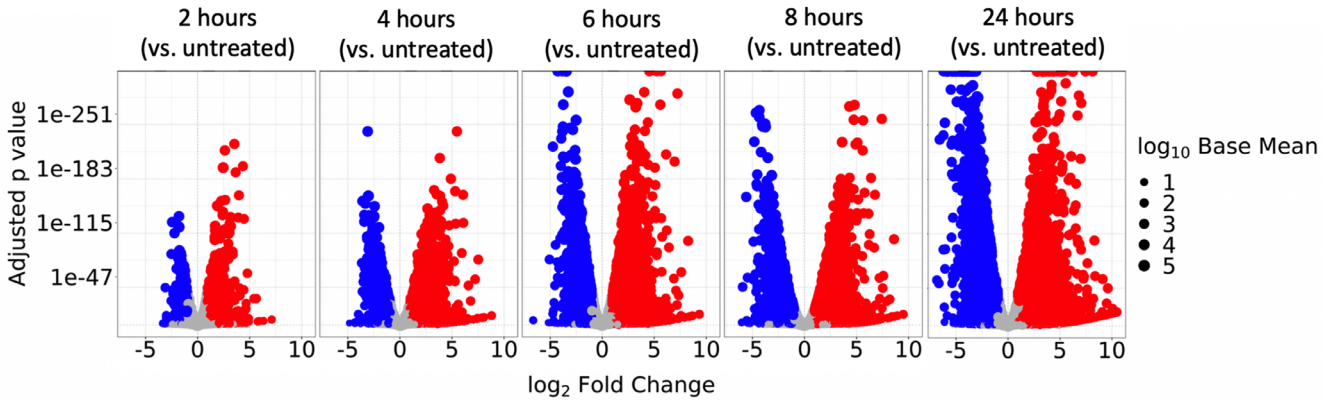

Figure 8. Gene expression changes following pan-HDAC inhibition. Volcano plot showing the increase in number of differentially expressed genes as a function of time following belinostat treatment. Gene expression levels were determined by RNA-seq. Note the relatively large fold-change in gene expression for many of these genes and the very high level of statistical significance.

least 5 half-lives. Of course, for the first 4 of those half-lives, the dose would actually be above the IC_{90} (by 16-fold, 8-fold, 4-fold, and 2-fold, sequentially). However, because our goal was not the eradication of 90% of tumor cells but rather 100%, we felt that these "excess" drug levels early following injection would actually be helpful and obviously cannot be avoided. We determined that 350 µg was the injection dose that achieved 2× IC_{90} on the far side of the vitreous for 5 half-lives, and therefore used 350 µg, as well as twice this value (700 µg) in subsequent in vivo experiments. The rabbit vitreous volume is half the size of a human child's vitreous volume, so experiments with intravitreal injections in rabbits generally have used a conversion factor of two when comparing with patients.[24,33–35] Thus, these calculated belinostat doses correspond to 700 µg and 1400 µg, respectively.

We have previously demonstrated that our vitreous seed and retinal tumor xenograft model,[25] which we originally based on prior work by Kang and Grossniklaus,[43] recapitulates the histopathologic findings of clinical disease seen in patients with RB. By using a xenograft model derived from human RB cells, we also increase the likelihood that the HDAC inhibition and cytotoxic efficacy seen in our model will translate to patients. In an effort to make our findings as clinically relevant as possible, we used a weekly dosing regimen, consistent with many clinical protocols.[3,12,16,44] From a practical point of view, any frequency greater than this would be impractical, as it would require unacceptably frequent anesthesia events for these young children. Several recent clinical treatment protocols for intravitreal injections with melphalan have decreased the frequency even further, to every 2 weeks or every 3 weeks, while maintaining good efficacy.[9,17,45] Less frequent belinostat dosing might likewise maintain the same excellent efficacy-to-toxicity ratio and therapeutic window seen here. Our protocol of three weekly injections did not eliminate 100% of tumor cells quantified in the vitreous. However, it should be noted that the efficacy of belinostat (95.5%) was numerically greater than, but statistically equivalent to ($P = 0.10$), current standard-of-care melphalan, and we know that melphalan is extremely effective at eradicating all tumor cells in patients. In addition, of the few live tumor cells still present 2 weeks after the third injection of belinostat, all were found to be positive on TUNEL staining, indicating that, although not quite dead yet, all had irreversibly already entered the process of apoptosis or necrosis, and none remained truly viable. This finding, taken together with the equivalent efficacy compared with melphalan in our experiments, suggests that all tumor cells can ultimately be eradicated by intravitreal belinostat.

Over the past decade, HDAC inhibitors have revolutionized the treatment of several different types of cancer, many of which had few good options previously. This has been especially true in the realm of liquid tumors, with HDAC inhibitors now approved by the US Food and Drug Administration (FDA) for the treatment of cutaneous T-cell lymphoma, peripheral T-cell lymphoma, and myeloma.[46,47] Belinostat itself is already approved for the treatment of patients with relapsed or refractory peripheral T-cell lymphoma.[48] However, the approach of using HDAC inhibitors for solid tumors has not been as successful,[47] notably including a trial of valproic acid for metastatic uveal melanoma that failed to demonstrate efficacy. HDAC inhibitors gradually alter histone acetylation to change chromatin structure and impact gene expression.[49,50] These generally require chronic exposure over time to cause these downstream changes in gene expression levels leading to cell death. In contrast, the pharmacokinetics of intravitreal injection,[51–53] with single injections spaced out over weeks, and the rapid decline in vitreous drug levels following each injection, would not be thought to be conducive to this sort of chronic sustained change in gene expression. It is possible that the efficacy seen in our in vivo experiments is due to sustained pharmacodynamics, even if the pharmacokinetics are brief. That is, the drug levels in the vitreous may rapidly decrease, but the drug may persist in having its effect on proteins inside the cell for a sustained period of time. Alternatively, the very high local concentrations achieved through intravitreal injection may overcome the need for chronic exposure, either by causing longer acting changes inside the cells or by activating other secondary targets or pathways (see below). In fact, some HDAC inhibitors known to have short half-lives still are able to cause longer duration effects on cells in vivo.[47]

Belinostat is a non-specific pan-HDAC inhibitor.[54] In fact, we found this same cytotoxicity against human RB cells to be a class effect, rather than specific to belinostat itself (data not shown). However, unlike most other FDA-approved HDAC inhibitors, belinostat is currently formulated in solution rather than as a pill taken orally. Thus, belinostat seemed the optimal choice within the HDAC inhibitor class to study via the intravitreal route, as it could be used in its current formulation. However, it is unclear which specific HDACs are being inhibited to mediate the cytotoxic effects seen in vivo. Certain HDACs are known to interact with pRB itself,[26,27] with other similar pocket proteins (e.g., p130)[28,29] or their binding partners,[30] and/or with other proteins important in RB pathways (e.g., E2F).[55] For example, both HDAC1 and HDAC3 have been reported to complex with pRB,[26,28,29] and both have been implicated in RB-dependent chromatin remodeling facilitating transcription at RB/E2F-responsive gene promoters.[29–31] In addition, HDACs are known to affect acetylation of histones (as their name implies) but also to have "off target" effects and cause acetylation changes in other (non-histone) proteins.[56–58] Effects on various critical cancer pathways, including those mediating apoptosis[59–61] and cell-cycle control,[62,63] have been shown to be caused in several ways: through direct complexing with pRB and other similar pocket proteins,[28] by impacting pRB complexes with other binding partners,[64] by regulating chromatin structure of RB-responsive downstream promoters,[29,31,55] by regulating transcription of other pRB binding partners themselves,[60] or by posttranslationally affecting acetylation and activation of RB pathway (and non-RB pathway) proteins. These conflicting data regarding the mechanisms of the various effects of HDAC on RB pathways goes back decades, and the complex interplay among these factors has never quite been teased out definitively.

Not surprisingly, the RNAseq gene expression experiments demonstrated that inhibition of HDACs 1 to 11 with the pan-HDAC inhibitor belinostat leads to widespread changes in gene expression, ultimately affecting thousands of genes. Our findings were consistent with previous findings regarding the effect of other pan-HDAC inhibitors in other cancer types,[40–42] both in terms of the specific gene sets being regulated and also in that both apoptotic and non-apoptotic pathways appear to be involved. Future studies should be directed to understanding the impact of inhibition of each of the specific HDACs and to determining which specific HDACs are required to be inhibited to mediate cell death in RB. These mechanistic experiments are currently ongoing, with the goal of maximizing specificity and mini-

mizing toxicity. Thus, although we demonstrated, for the first time to the best of our knowledge, that belinostat is an attractive clinical therapy for treating recalcitrant vitreous seeds by intravitreal injection in vivo in our animal model, the physiological underpinnings of this emerging therapy for RB remain to be fully elucidated. Future clinical trials could directly evaluate the benefit of this therapy in patients with RB and vitreous seeds.

Conclusions

Our in vivo experiments demonstrate that the HDAC inhibitor belinostat is equally effective as current standard-of-care melphalan in eradicating retinoblastoma vitreous seeds, but without the retinal toxicity seen with melphalan. This suggests that belinostat may be an attractive agent to pursue in future clinical trials.

Acknowledgments

Supported by a grant from the National Eye Institute, National Institutes of Health (K08EY027464 to ABD); by a Career Development Award from the Research to Prevent Blindness Foundation (ABD); by an unrestricted departmental grant from Research to Prevent Blindness to the Vanderbilt Department of Ophthalmology and Visual Sciences; by a Department of Veterans Affairs Senior Research Career Scientist Award (AR); by a Vanderbilt-Ingram Cancer Center Support grant for core facilities (CA68485); by a grant from the National Institute of General Medical Sciences, National Institutes of Health (P41 GM103391-06); and by a grant from the National Center for Research Resources (UL1RR024975-01; now at the National Center for Advancing Translational Sciences, 2 UL1TR000445-06). The content is the sole responsibility of the authors and does not necessarily represent the official views of the National Institutes of Health. Research funding, as well as the Evomela and Belinostat, were provided by Spectrum Pharmaceuticals, Inc., as part of an investigator-initiated study. Spectrum Pharmaceuticals, Inc., was not involved in the design or performance of the experiments or in the data analysis, and they did not have editorial or veto control over the data or its publication.

Portions of this work were presented at the International Society of Ocular Oncology Meeting in 2019 (Los Angeles, CA), at the ARVO Annual Meeting in 2019 (Vancouver, BC, Canada), at the Macula Society Annual Meeting in 2019 (Bonita Springs, FL), and at the American Academy of Ocular Oncology and Pathology Annual Meeting in 2019 (San Francisco, CA).

Disclosure: **J.V. Kaczmarek**, None; **C.M. Bogan**, None; **J.M. Pierce**, None; **Y.K. Tao**, Duke University (P), Leica Microsystems (F); **S.-C. Chen**, None; **Q. Liu**, None; **X. Liu**, None; **K.L. Boyd**, None; **M.W. Calcutt**, None; **T.M. Bridges**, None; **C.W. Lindsley**, None; **D.L. Friedman**, Vanderbilt University Medical Center (P); **A. Richmond**, None; **A.B. Daniels**, Vanderbilt University Medical Center (P)

References

1. Abramson DH, Dunkel IJ, Brodie SE, Kim JW, Gobin YP. A phase I/II study of direct intraarterial (ophthalmic artery) chemotherapy with melphalan for intraocular retinoblastoma initial results. *Ophthalmology.* 2008;115(8):1398–1404, 1404.e1.
2. Munier FL, Soliman S, Moulin AP, Gaillard MC, Balmer A, Beck-Popovic M. Profiling safety of intravitreal injections for retinoblastoma using an anti-reflux procedure and sterilisation of the needle track. *Br J Ophthalmol.* 2012;96(8):1084–1087.
3. Munier FL, Gaillard MC, Balmer A, Beck-Popovic M. Intravitreal chemotherapy for vitreous seeding in retinoblastoma: recent advances and perspectives. *Saudi J Ophthalmol.* 2013;27(3):147–150.
4. Shields CL, Mashayekhi A, Au AK, et al. The International Classification of Retinoblastoma predicts chemoreduction success. *Ophthalmology.* 2006;113(12):2276–2280.
5. Shields CL, Honavar SG, Meadows AT, et al. Chemoreduction plus focal therapy for retinoblastoma: factors predictive of need for treatment with external beam radiotherapy or enucleation. *Am J Ophthalmol.* 2002;133(5):657–664.
6. Abramson DH, Daniels AB, Marr BP, et al. Intra-arterial chemotherapy (ophthalmic artery chemosurgery) for group D retinoblastoma. *PLoS One.* 2016;11(1):e0146582.
7. Daniels AB, Patel SN, Milam RW, Kohanim S, Friedman DL, Koyama T. Effect of intravenous chemotherapy regimen on globe salvage success rates for retinoblastoma based on disease Class-A meta-analysis. *Cancers (Basel).* 2021;13(9):2216.
8. Yuan S, Friedman DL, Daniels AB. Evolution of chemotherapy approaches for the treatment of intraocular retinoblastoma: a comprehensive review. *Int Ophthalmol Clin.* 2017;57(1):117–128.
9. Francis JH, Iyer S, Gobin YP, Brodie SE, Abramson DH. Retinoblastoma vitreous seed clouds (class 3): a comparison of treatment with ophthalmic artery chemosurgery with or without intravitreous and periocular chemotherapy. *Ophthalmology.* 2017;124(10):1548–1555.
10. Berry JL, Shah S, Bechtold M, Zolfaghari E, Jubran R, Kim JW. Long-term outcomes of Group D retinoblastoma eyes during the intravitreal melphalan era. *Pediatr Blood Cancer.* 2017;64(12):e26696.
11. Francis JH, Abramson DH, Gaillard MC, Marr BP, Beck-Popovic M, Munier FL. The classification of vitreous seeds in retinoblastoma and response to intravitreal melphalan. *Ophthalmology.* 2015;122(6):1173–1179.
12. Berry JL, Bechtold M, Shah S, et al. Not all seeds are created equal: seed classification is predictive of outcomes in retinoblastoma. *Ophthalmology.* 2017;124(12):1817–1825.
13. Shields CL, Douglass AM, Beggache M, Say EA, Shields JA.Intravitreous chemotherapy for active vitreous seeding from retinoblastoma: outcomes after 192 consecutive injections. The 2015 Howard Naquin Lecture. *Retina.* 2016;36(6):1184–1190.
14. Daniels AB, Froehler MT, Nunnally AH, et al. Rabbit model of intra-arterial chemotherapy toxicity demonstrates retinopathy and vasculopathy related to drug and dose, not procedure or approach. *Invest Ophthalmol Vis Sci.* 2019;60(4):954–964.
15. Tse BC, Steinle JJ, Johnson D, Haik BG, Wilson MW. Superselective intraophthalmic artery chemotherapy in a nonhuman primate model: histopathologic findings. *JAMA Ophthalmol.* 2013;131(7):903–911.
16. Francis JH, Schaiquevich P, Buitrago E, et al. Local and systemic toxicity of intravitreal melphalan for vitreous seeding in retinoblastoma: a preclinical and clinical study. *Ophthalmology.* 2014;121(9):1810–1817.
17. Xue K, Ren H, Meng F, Zhang R, Qian J. Ocular toxicity of intravitreal melphalan for retinoblastoma in Chinese patients. *BMC Ophthalmol.* 2019;19(1):61.
18. Ghassemi F, Amoli FA. Pathological findings in enucleated eyes after intravitreal melphalan injection. *Int Ophthalmol.* 2014;34(3):533–540.
19. Yuan S, Friedman DL, Daniels AB. Alternative chemotherapeutic agents for the treatment of retinoblastoma using the intra-arterial and intravitreal routes: a path forward toward drug discovery. *Int Ophthalmol Clin.* 2017;57(1):129–141.

20. Mohney BG, Elner VM, Smith AB, et al. Preclinical acute ocular safety study of combined intravitreal carboplatin and etoposide phosphate for retinoblastoma. *Ophthalmic Surg Lasers Imaging Retina.* 2017;48(2):151–159.
21. Smith SJ, Pulido JS, Salomao DR, Smith BD, Mohney B. Combined intravitreal and subconjunctival carboplatin for retinoblastoma with vitreous seeds. *Br J Ophthalmol.* 2012;96(8):1073–1077.
22. Nadelmann J, Francis JH, Brodie SE, Muca E, Abramson DH. Is intravitreal topotecan toxic to retinal function? *Br J Ophthalmol.* 2021;105(7):1016–1018.
23. Rao R, Honavar SG, Sharma V, Reddy VAP. Intravitreal topotecan in the management of refractory and recurrent vitreous seeds in retinoblastoma. *Br J Ophthalmol.* 2018;102(4):490–495.
24. Bogan CM, Kaczmarek JV, Pierce JM, et al. Evaluation of intravitreal topotecan dose levels, toxicity and efficacy for retinoblastoma vitreous seeds: a preclinical and clinical study [published online ahead of print May 10, 2021]. *Br J Ophthalmol,* https://doi.org/10.1136/bjophthalmol-2020-318529.
25. Daniels AB, Froehler MT, Pierce JM, et al. Pharmacokinetics, tissue localization, toxicity, and treatment efficacy in the first small animal (rabbit) model of intra-arterial chemotherapy for retinoblastoma. *Invest Ophthalmol Vis Sci.* 2018;59(1):446–454.
26. Fajas L, Egler V, Reiter R, et al. The retinoblastoma-histone deacetylase 3 complex inhibits PPARgamma and adipocyte differentiation. *Dev Cell.* 2002;3(6):903–910.
27. Takaki T, Fukasawa K, Suzuki-Takahashi I, Hirai H. Cdk-mediated phosphorylation of pRB regulates HDAC binding in vitro. *Biochem Biophys Res Commun.* 2004;316(1):252–255.
28. Stiegler P, De Luca A, Bagella L, Giordano A. The COOH-terminal region of pRb2/p130 binds to histone deacetylase 1 (HDAC1), enhancing transcriptional repression of the E2F-dependent cyclin A promoter. *Cancer Res.* 1998;58(22):5049–5052.
29. Ferreira R, Magnaghi-Jaulin L, Robin P, Harel-Bellan A, Trouche D. The three members of the pocket proteins family share the ability to repress E2F activity through recruitment of a histone deacetylase. *Proc Natl Acad Sci USA.* 1998;95(18):10493–10498.
30. Gray SG, Iglesias AH, Lizcano F, et al. Functional characterization of JMJD2A, a histone deacetylase- and retinoblastoma-binding protein. *J Biol Chem.* 2005;280(31):28507–28518.
31. Siddiqui H, Solomon DA, Gunawardena RW, Wang Y, Knudsen ES. Histone deacetylation of RB-responsive promoters: requisite for specific gene repression but dispensable for cell cycle inhibition. *Mol Cell Biol.* 2003;23(21):7719–7731.
32. Di Fiore R, D'Anneo A, Tesoriere G, Vento R. RB1 in cancer: different mechanisms of RB1 inactivation and alterations of pRb pathway in tumorigenesis. *J Cell Physiol.* 2013;228(8):1676–1687.
33. Daniels AB, Pierce JM, Chen SC. Complete preclinical platform for intravitreal chemotherapy drug discovery for retinoblastoma: assessment of pharmacokinetics, toxicity and efficacy using a rabbit model. *MethodsX.* 2021;8:101358.
34. Oatess TL, Chen PH, Daniels AB, Himmel LE. Severe periocular edema after intraarterial carboplatin chemotherapy for retinoblastoma in a rabbit (*Oryctolagus cuniculus*) model. *Comp Med.* 2020;70(2):176–182.
35. Bogan CM, Pierce JM, Doss SD, et al. Intravitreal melphalan hydrochloride vs propylene glycol-free melphalan for retinoblastoma vitreous seeds: efficacy, toxicity and stability in rabbits models and patients. *Exp Eye Res.* 2021;204:108439.
36. Bozic I, Li X, Tao Y. Quantitative biometry of zebrafish retinal vasculature using optical coherence tomographic angiography. *Biomed Opt Express.* 2018;9(3):1244–1255.
37. Gjorloff K, Andreasson S, Ehinger B. Standardized full-field electroretinography in rabbits. *Doc Ophthalmol.* 2004;109(2):163–168.
38. Newbold A, Falkenberg KJ, Prince HM, Johnstone RW. How do tumor cells respond to HDAC inhibition? *FEBS J.* 2016;283(22):4032–4046.
39. Mrakovcic M, Kleinheinz J, Frohlich LF. p53 at the crossroads between different types of HDAC inhibitor-mediated cancer cell death. *Int J Mol Sci.* 2019;20(10):2415.
40. Heller G, Schmidt WM, Ziegler B, et al. Genome-wide transcriptional response to 5-aza-2′-deoxycytidine and trichostatin a in multiple myeloma cells. *Cancer Res.* 2008;68(1):44–54.
41. Sato N, Fukushima N, Maitra A, et al. Discovery of novel targets for aberrant methylation in pancreatic carcinoma using high-throughput microarrays. *Cancer Res.* 2003;63(13):3735–3742.
42. Zhong S, Fields CR, Su N, Pan YX, Robertson KD. Pharmacologic inhibition of epigenetic modifications, coupled with gene expression profiling, reveals novel targets of aberrant DNA methylation and histone deacetylation in lung cancer. *Oncogene.* 2007;26(18):2621–2634.
43. Kang SJ, Grossniklaus HE. Rabbit model of retinoblastoma. *J Biomed Biotechnol.* 2011;2011:394730.
44. Brodie SE, Pierre Gobin Y, Dunkel IJ, Kim JW, Abramson DH. Persistence of retinal function after selective ophthalmic artery chemotherapy infusion for retinoblastoma. *Doc Ophthalmol.* 2009;119(1):13–22.
45. Berry JL, Shah S, Kim F, Jubran R, Kim JW. Integrated treatment during the intravitreal melphalan era: concurrent intravitreal melphalan and systemic chemoreduction. *Ocul Oncol Pathol.* 2018;4(6):335–340.
46. Shah RR. Safety and tolerability of histone deacetylase (HDAC) inhibitors in oncology. *Drug Saf.* 2019;42(2):235–245.
47. McClure JJ, Li X, Chou CJ. Advances and challenges of HDAC inhibitors in cancer therapeutics. *Adv Cancer Res.* 2018;138:183–211.
48. Lee HZ, Kwitkowski VE, Del Valle PL, et al. FDA approval: belinostat for the treatment of patients with relapsed or refractory peripheral T-cell lymphoma. *Clin Cancer Res.* 2015;21(12):2666–2670.
49. Li W, Sun Z. Mechanism of action for HDAC inhibitors-insights from omics approaches. *Int J Mol Sci.* 2019;20(7):1616.
50. Stengel KR, Bhaskara S, Wang J, et al. Histone deacetylase 3 controls a transcriptional network required for B cell maturation. *Nucleic Acids Res.* 2019;47(20):10612–10627.
51. Schaiquevich P, Fabius AW, Francis JH, Chantada GL, Abramson DH. Ocular pharmacology of chemotherapy for retinoblastoma. *Retina.* 2017;37(1):1–10.
52. Buitrago E, Winter U, Williams G, Asprea M, Chantada G, Schaiquevich P. Pharmacokinetics of melphalan after intravitreal injection in a rabbit model. *J Ocul Pharmacol Ther.* 2016;32(4):230–235.
53. Buitrago E, Hocht C, Chantada G, et al. Pharmacokinetic analysis of topotecan after intra-vitreal injection. Implications for retinoblastoma treatment. *Exp Eye Res.* 2010;91(1):9–14.
54. Roche J, Bertrand P. Inside HDACs with more selective HDAC inhibitors. *Eur J Med Chem.* 2016;121:451–483.
55. Lu Z, Luo RZ, Peng H, et al. E2F-HDAC complexes negatively regulate the tumor suppressor gene ARHI in breast cancer. *Oncogene.* 2006;25(2):230–239.
56. Choudhary C, Weinert BT, Nishida Y, Verdin E, Mann M. The growing landscape of lysine acetylation links metabolism

Investigative Ophthalmology & Visual Science

and cell signalling. *Nat Rev Mol Cell Biol.* 2014;15(8):536–550.

57. Spange S, Wagner T, Heinzel T, Kramer OH. Acetylation of non-histone proteins modulates cellular signalling at multiple levels. *Int J Biochem Cell Biol.* 2009;41(1):185–198.
58. Jeong Y, Du R, Zhu X, et al. Histone deacetylase isoforms regulate innate immune responses by deacetylating mitogen-activated protein kinase phosphatase-1. *J Leukoc Biol.* 2014;95(4):651–659.
59. Wagner S, Roemer K. Retinoblastoma protein is required for efficient colorectal carcinoma cell apoptosis by histone deacetylase inhibitors in the absence of p21Waf. *Biochem Pharmacol.* 2005;69(7):1059–1067.
60. Tan J, Zhuang L, Jiang X, Yang KK, Karuturi KM, Yu Q. Apoptosis signal-regulating kinase 1 is a direct target of E2F1 and contributes to histone deacetylase inhibitor-induced apoptosis through positive feedback regulation of E2F1 apoptotic activity. *J Biol Chem.* 2006;281(15):10508–10515.
61. Kim JK, Kan G, Mao Y, et al. UHRF1 downmodulation enhances antitumor effects of histone deacetylase inhibitors in retinoblastoma by augmenting oxidative stress-mediated apoptosis. *Mol Oncol.* 2020;14(2):329–346.
62. Baumann P, Junghanns C, Mandl-Weber S, Strobl S, Oduncu F, Schmidmaier R. The pan-histone deacetylase inhibitor CR2408 disrupts cell cycle progression, diminishes proliferation and causes apoptosis in multiple myeloma cells. *Br J Haematol.* 2012;156(5):633–642.
63. Chuang JY, Hung JJ. Overexpression of HDAC1 induces cellular senescence by Sp1/PP2A/pRb pathway. *Biochem Biophys Res Commun.* 2011;407(3):587–592.
64. Suryadinata R, Sadowski M, Steel R, Sarcevic B. Cyclin-dependent kinase-mediated phosphorylation of RBP1 and pRb promotes their dissociation to mediate release of the SAP30.mSin3.HDAC transcriptional repressor complex. *J Biol Chem.* 2011;286(7):5108–5118.